# Design and experiment of the soil-covering and soil-compacting device for seedling raising and sowing of trough type panax notoginseng

Wencai Yang[1*], Wang Pu[1], Lulu Xu[2], Ziyuan Tian[1], Jing Zhao[1], Yijie Zhang[1], Zhenjie Yang[1]
(1. *College of Mechanical and Electrical Engineering, Yunnan Agricultural University, Kunming 650201, China*;
2. *Agricultural and rural Bureau, Southwest Guizhou 562499, China*)

**Abstract:** In order to improve the seedling quality of Panax notoginseng, combined with the special agronomic requirements of Panax notoginseng, a sharp angle roller soil-covering and soil-compacting device integrating the functions of soil-covering and soil-compacting was designed. Based on the theoretical analysis of seed ditch conditions, soil-covering process and soil-compacting process, the structure of soil-covering and soil-compacting device was designed. Through theoretical analysis and calculation, the diameter and length of soil-covering and soil-compacting wheel were 20 cm and 10.7-14.1 cm, respectively, the sharp angle and height range were 45°-105° and 0.8-1.6 cm respectively, and the spring stiffness was 38.54 N/mm; Using the discrete element method to simulate the soil-covering and soil-compacting process, it was obtained that when the sharp angle range was 60°-90°, the sharp angle height range was 0.8-1.2 cm, and the soil-covering effect was better; Taking the forward speed, ballast pressure, sharp angle and sharp angle height of the planter as the test factors, and taking the soil-covering thickness, grain spacing and soil compactness as the indexes, the four factor and three-level Box-Behnken Design test was carried out. The response surface test analysis method was used to establish the regression equation between the factors and indexes, and determine the best parameter combination: the forward speed was 6.5 m/min, the ballast pressure was 360.5 N, the sharp angle was 67°, and the sharp angle height was 1 cm, at this time, the soil-covering thickness was 0.64 cm, the grain spacing was 5.03 cm, and the soil compactness was 321.77 kPa. According to the soil trough test, the design of soil-covering and soil-compacting device met the agronomic requirements of plant spacing, soil-compactness and soil-covering thickness during seedling sowing of Panax notoginseng. The research results can provide a reference for the design of Panax notoginseng seedling planter integrating pressing hole (ditching), sowing, soil-covering and soil-compacting.
**Keywords:** Panax notoginseng, trough type, seedling raising and sowing, soil-covering and soil-compacting, EDEM, test
**DOI:** 10.25165/j.ijabe.20231605.7606

**Citation:** Yang W C, Pu W, Xu L L, Tian Z Y, Zhao J, Zhang Y J, et al. Design and experiment of the soil-covering and soil-compacting device for seedling raising and sowing of trough type panax notoginseng. Int J Agric & Biol Eng, 2023; 16(5): 113–122.

## 1 Introduction

Panax notoginseng is a famous Chinese herbal medicine in Yunnan Province. It is an important raw material for cosmetics and health products. It has a large market demand and good development prospects. At present, the total area of Panax notoginseng in Yunnan has reached 151.3 km$^2$, and the planting sales revenue of Panax notoginseng has reached 10.3 billion CNY, accounting for 35% of the total planting sales revenue of traditional Chinese medicine in the province[1]. The seedling raising of Panax notoginseng is generally carried out in the trough. The seedling raising time is up to 1 a. The sowing agronomy is special. The row plant spacing is 5 cm, the sowing depth is about 1 cm, and the matrix compactness is 200-400 kPa[2]. The basic procedures of seedling raising and sowing of Panax notoginseng are: land preparation, ridging, hole pressing (or trenching), spot sowing, soil-covering and soil-compacting. At present, the degree of mechanization is relatively low. After land preparation and ridging, a small number of semi mature planters can only solve the two procedures of hole pressing and sowing, and the qualified rate of sowing is low. In particular, the links of soil-covering and soil-compacting completely rely on labor, which has low efficiency, high labor intensity and high cost, Moreover, the uniformity of the soil-covering thickness and soil compactness is poor due to human error. The quality of soil-covering and soil-compacting operation is one of the keys to ensure the seedling quality of Panax notoginseng. The soil-covering and soil-compacting device is the main soil touching part of the planter to realize the soil-covering and soil-compacting of seeds and play the role of increasing, preserving and supplying soil moisture[3-8]. However, there is still a lack of research and development on the soil-covering and soil-compacting device for Panax notoginseng seedling sowing. The current manual method cannot meet the agronomic requirements of soil-covering and soil-compacting operation for Panax notoginseng seedling sowing with shallow sowing depth and small row plant spacing. Therefore, designing a soil-covering and soil-compacting device suitable for Panax notoginseng sowing agronomy is of great significance to the cultivation of high-quality Panax notoginseng seedlings.

At present, the soil-covering and soil-compacting devices have

**Received date:** 2022-04-18 **Accepted date:** 2023-08-31
**Biographies: Wang Pu**, MS candidate, research interest: agricultural mechanization engineering, Email: wo1556685469@163.com; **Lulu Xu**, MS, research interest: agricultural mechanization engineering, Email: 2387097490@qq.com; **Ziyuan Tian**, MS, research interests: agricultural mechanization engineering, Email: 1120772126@qq.com; **Jing Zhao**, MS, research interest: agricultural mechanization engineering, Email: 2311956046@qq.com; **Yijie Zhang**, Associate Professor, research interest: agricultural plant protection machinery, Email: 562525920@qq.com; **Zhenjie Yang**, PhD, research interest: agricultural machinery equipment, Email: yangzj@ynau.edu.cn.
***Corresponding author: Wencai Yang**, PhD, Professor, research interest: agricultural mechanization and equipment engineering. College of Mechanical and Electrical Engineering, Yunnan Agricultural University, Kunming 650201, China. Tel:+86-15887294829, Email: yangwencai2005@126.com.

two structures: split type and integrated type. The basic structure of the split soil-covering part mainly includes scraper soil-covering device, double disc soil-covering device, throwing soil-covering device and bionic soil-covering device[9-11]; Zheng et al.[12] designed a soil-covering device with linkage and differential adjustment to solve the problems of inconsistent soil-covering volume on both sides of slope and inconvenient adjustment of soil-covering plate, which could ensure uniform and stable soil-covering; Li et al.[13] designed a disc type soil-covering device and a roller type soil-compacting wheel according to the agronomic requirements of deep planting and shallow covering of sugarcane. In the process of soil-covering and soil-compacting, the soil-covering thickness was uniform and did not block the soil; The soil-compacting part was mainly a viscosity reducing and drag reducing soil-compacting device based on the principles of bionics, scraping and vibration[14-16]; The integrated soil-covering and soil-compacting included four structures: plane, concave, convex and conical. V-shaped and elastic spiral soil-covering and soil-compacting devices were designed[17]. Koichiro et al.[18] designed a vibration soil-compacting device that could adjust different working modes to realize multiple functions of one machine. The existing soil-covering and soil-compacting device was mainly aimed at the crops with large row spacing in the field, which had a large disturbance to the soil and seeds, and could not meet the agronomic requirements of Panax notoginseng seedling cultivation and sowing with shallow sowing depth and small row spacing. Therefore, according to the agronomic requirements of seedling raising and sowing of Panax notoginseng, a sharp angle roller soil-covering and soil-compacting device was designed to reduce the disturbance to soil and seeds and improved the operation effect.

Different structural parameters of soil-covering and soil-compacting device have different disturbance to soil and seeds[19-21]. The simulation method is often used to study the disturbance process of soil contacting parts-soil-seed, and the common methods are finite element method and discrete element method. The finite element method is mainly used to study the mutual movement law between the soil contacting parts and the soil, the stress and deformation of the soil, and is suitable for studying the operation processes such as subsoiling and hole pressing[22,23]; The discrete element method can effectively simulate the micro and macro deformation between soil particles and soil contacting parts, and can intuitively reflect the interaction and movement process of soil contacting parts, soil particles and seeds. It is suitable for studying the process of soil-covering and soil-compacting[24-26]. Therefore, in this study, the discrete element method was used to simulate the process of soil-covering and soil-compacting.

According to the agronomic characteristics of shallow sowing depth and dense plants of Panax notoginseng, a sharp angle roller type soil-covering and soil-compacting device was designed in this paper. The key structural parameters were designed through the dynamic analysis of the process of soil-covering and soil-compacting; Using the discrete element method, according to the effect of soil-covering and soil-compacting, the sharp height and angle parameter range of soil-covering and soil-compacting wheel were studied; Taking the forward speed, ballast pressure, sharp angle and height of the planter as the experimental factors, and taking the soil-covering thickness, grain spacing and soil compactness as the indexes, the best parameter combination was studied through the soil trough test to verify whether it met the agronomic requirements of Panax notoginseng seedling cultivation and sowing.

## 2 Structural design of soil-covering and soil-compacting device

### 2.1 Overall structure and working principle

The soil-covering and soil-compacting device was mainly composed of frame, motor, compression spring, soil-covering and soil-compacting wheel connecting frame and soil-covering and soil-compacting wheel, as shown in Figure 1. Because the matrix in the seedling trough for Panax notoginseng seedling sowing was uneven horizontally and vertically, in order to increase the profiling effect and ensure the uniform soil-covering and soil-compacting, the soil-covering and soil-compacting wheel was combined in sections. Considering the factors such as the width of the seedling trough, the spacing of seed ditches and the soil-covering thickness, the soil-covering and soil-compacting device was divided into four sections, and each section could cover and suppress seven rows of seed ditches. The soil-covering and soil-compacting wheel was connected with the seeding machine through the installation shaft and the ballast pressure regulating structure. The seeding machine was self-propelled and the power was provided by the motor.

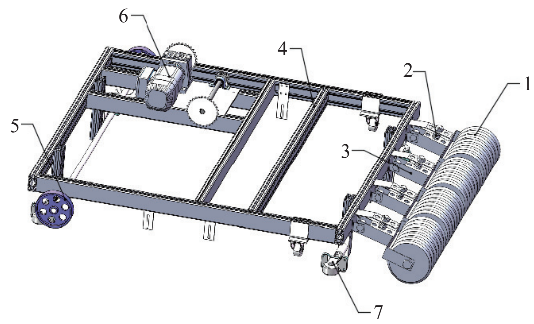


1. Soil-covering and soil-compacting wheel 2. Ballast pressure regulator 3. Fixing frame of soil-covering and soil-compacting wheel 4. Rack 5. Traveling wheel 6. Motor 7. Limit wheel

Figure 1 Overall structure of soil-covering and soil-compacting device

Working principle of soil-covering and soil-compacting: during operation, the soil-covering and soil-compacting wheel rolls forwarded with the planter and carried out soil-covering and soil-compacting under the action of self weight and ballast pressure regulating structure. The process of soil-covering and soil-compacting is shown in Figure 2. Two adjacent sharp angles of the soil-covering and soil-compacting wheel formed a trapezoidal section with the surface of the drum. During the operation, the soil particles fell into the seed ditch under the action of the sharp angle extrusion force $F_T$, and the pressing operation was completed under the joint action of the sharp angle and the surface of the drum. The squeezing force $F_T$ of sharp angle on soil particles should point to the seed ditch, which was affected by the height and angle of sharp angle.

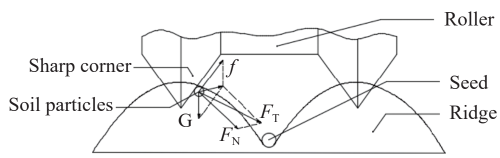


Note: $G$ is the self weight of soil particles, N; $F_N$ is the supporting force of soil particles by the soil-covering and soil-compacting wheel, N; $f$ is the friction force of soil particles subjected to the soil-covering and soil-compacting wheel, N; $F_T$ is the synthetic force of each force, N.

Figure 2 Schematic diagram of soil-covering and soil-compacting

### 2.2 Theoretical analysis of soil-covering and soil-compacting

#### 2.2.1 Ridge contour curve fitting

The soil movement during soil-covering and soil-compacting was related to the structure of soil-covering and soil-compacting wheel and the shape of seed ditch, and the structure of soil-covering and soil-compacting wheel needed to be coordinated with the shape of ridge, so the contour curve of ridge shape was fitted. The soil in the seedling trough was finely crushed and leveled. After the soil moisture content was adjusted to 20%-30%, the seed ditch was opened through the ditching device and the cross-section of the seed ditch was cut. The coordinate marking paper was used to fit and contact with the cross-section, and the seed ditch contour (Ridge) was obtained by light projection of the contour shape of the seed ditch. The fitting curve and equation are shown in Figure 3.

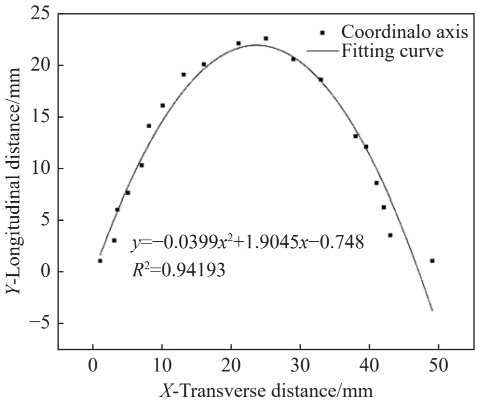


Figure 3 Curve fitting of seed furrow contour (ridge)

#### 2.2.2 Analysis of covered soil area

A good soil-covering and soil-compacting operation should have small disturbance to the seeds of Panax notoginseng, high consistency of soil-covering thickness, and make the seeds reasonably close to the soil, which was conducive to the germination and growth of Panax notoginseng seeds. In the process of soil-covering and soil-compacting, the sharp angles pressed the soil on both sides into the seed ditch, and the soil-compacting parts pressed at the same time. After the soil-covering and soil-compacting, a trapezoidal section was formed. According to the ridge contour extracted above, the soil state and seed position after soil-covering and soil-compacting are shown in Figure 4.

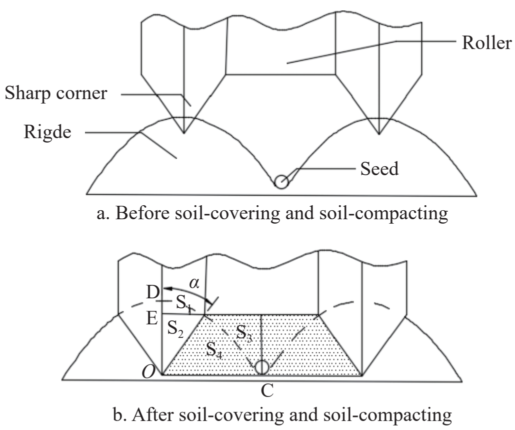


Figure 4 Schematic diagram of seeds and soil after soil-covering and soil-compacting

The amount of soil to be covered was the amount of soil squeezed into the seed ditch by the sharp angle of the soil-covering and soil-compacting wheel. The more the amount of soil covered, the deeper the thickness of the soil covered. The amount of covering soil was related to the angle, height and spacing of sharp angles. After the covering soil was compacted, the trapezoidal cross-sectional area should be less than the ridge contour area, that is:

$$\begin{cases} S_1+S_2+S_4>S_3+S_4 \\ S_1+S_2+S_4=\int_{x_D}^{x_C} f(x)\mathrm{d}x \\ S_3+S_4=2.5\times|OE|-\dfrac{1}{2}|OE|^2\tan\alpha \\ f(x)=-0.0399x^2+1.9045x-0.748 \end{cases} \tag{1}$$

where, $\alpha$ is the sharp angle of the soil-covering and soil-compacting wheel, (°); |OE| is the height of the soil-covering and soil-compacting wheel, cm; $x_C$ and $x_D$ are the coordinate values of point $C$ and point $D$ in Figure 4; $S_1$, $S_2$, $S_3$ and $S_4$ are the area of each region in Figure 4, and $f(x)$ is the fitting equation of the ridge.

From the above equation:

$$2.5\times|OE|-\frac{1}{2}|OE|^2\tan\alpha<\int_{x_D}^{x_C} f(x)\mathrm{d}x \tag{2}$$

Through the analysis of Equation (2), it could be seen that the amount of soil covered was related to the sharp angle, the sharp angle height and the contour shape of the seed ditch. When the sharp angle height is different, it could be seen that the soil-covering thickness and compactness of the seeds will also change. If the sharp angle height was greater than the depth of the seed ditch, the soil-covering and soil-compacting wheel would not suppress the soil above the seeds. If the sharp angle height was less than the maximum diameter of Panax notoginseng seeds, the amount of covered soil would be reduced, and a large ballast pressure would be generated on the seeds and the soil above the seeds, and even backwater would be generated. Therefore, it was inferred that the sharp angle height would affect the amount of covered soil and soil compactness after compaction by the soil-covering and soil-compacting wheel.

#### 2.2.3 Analysis of soil-compacting principle

During soil-covering and soil-compacting, the soil on the planting ditch bears the ballast pressure exerted by the soil-covering and soil-compacting wheel, so as to complete the soil-compacting operation. The soil-compacting operation should meet the soil compactness required by the agronomy of Panax notoginseng seedling and sowing. The soil compactness was related to the grounding area and ballast pressure of the soil-covering and soil-compacting wheel. The ballast pressure was determined by the gravity and profiling adjustment force of the soil-covering and soil-compacting wheel, and the grounding area was determined by the roller radius and sharp angle and height, etc. Since the soil-covering and soil-compacting wheel had the same effect on adjacent seed ditches, the soil-covering and soil-compacting wheel of 2 rows of seed ditches was intercepted for research, and its grounding area was shown in the shaded part in Figure 5.

When the rigid wheel was in contact with the rigid road surface, the width of the rigid wheel could be expressed by its radial contact area[27]. Therefore, its area could be approximately the area of the ring, and the grounding area $S$ of the soil-covering and soil-compacting wheel is:

$$S=\frac{\beta\pi R}{180}(B-3b)b+3\times\frac{2\beta\pi\left[(R+h)^2-R^2\right]}{360\cos\dfrac{\alpha}{2}} \tag{3}$$

where, $R$ is the radius of the soil-covering and soil-compacting wheel, cm; $\beta$ is the subsidence angle, (°); $\alpha$ is the Sharp angle, (°); $h$

is the height of sharp angle, cm; $b$ is the width of sharp angle, cm; $B$ is the length of the soil-covering and soil-compacting wheel, cm.

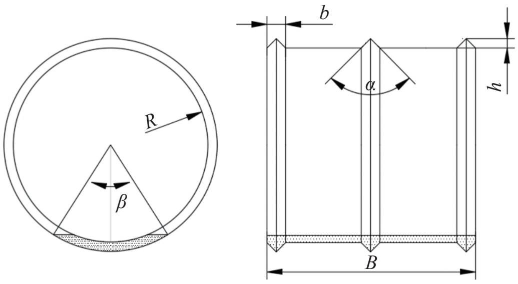


a. Left view b. Front view

Note: $R$ is the radius of the soil-covering and soil-compacting wheel, cm; $\beta$ Is the subsidence angle, (°); $\alpha$ Sharp angle, (°); $h$ is the height of sharp angle, cm; $b$ is the width of sharp angle, cm; $B$ is the length of the soil-covering and soil-compacting wheel, cm.

Figure 5 Schematic diagram of soil contact area

During operation, the deformation of the outer wall of the soil-covering and soil-compacting wheel under the action of soft soil was very small, so its deformation could be ignored. The soil-covering and soil-compacting wheel could regard it as a rigid body, and simplified the lateral flow of the soil below the contact surface between the soil-covering and soil-compacting wheel and the soil, so the soil stress on the center and both sides of the contact surface could be regarded as uniform distribution, and its grounding pressure $p$ is:

$$p = \frac{Q}{S} \tag{4}$$

where, $Q$ is the ballast pressure. According to the requirements of Panax notoginseng agriculture, the soil compactness is 200-400 kPa[2]. Combined with Equations (3) and (4), the grounding pressure of soil-covering and soil-compacting wheel shall meet:

$$200\text{ kPa} < \frac{Q}{\frac{\beta\pi(R-h)}{180}\left(B-3\text{b}\right)+3\frac{2\beta\pi\left[R^2-(R-h)^2\right]}{360\cos\frac{\alpha}{2}}} < 400\text{ kPa} \tag{5}$$

It could be seen from the above equation that the ballast pressure was related to the diameter, sharp angle height and sharp angle of the soil-covering and soil-compacting wheel. Under the condition that the sharp angle height and angle remain unchanged, in order to meet the requirements of soil-compacting pressure and control the cost, a smaller direct diameter of the soil-covering and soil-compacting wheel should be selected within the range of agronomic requirements.

## 2.3 Structural parameter design

### 2.3.1 Diameter design

The soil-covering and soil-compacting wheel was a sharp angle roller structure. The soil-covering and soil-compacting operation was completed by sharp angle extrusion and roller rotation. The operation quality was related to the sharp angle height, sharp angle and the diameter of the soil-covering and soil-compacting wheel. The smaller the diameter of the soil-covering and soil-compacting wheel, the greater the slip rate in the operation. At the same time, it was easy to block the soil, which directly affected the soil-covering thickness, the grain spacing and the soil compactness effect. On the contrary, the larger the diameter of the soil-covering and soil-compacting wheel was, the easier the drum was to rotate, which could reduce the slip rate and soil blocking phenomenon in the process of operation, but the excessive diameter would increase the rolling resistance in the process of operation [10]. In order to meet the normal rolling of the soil-covering and soil-compacting wheel, its diameter should meet[17]:

$$D \geq \frac{2W_r}{Qf} \tag{6}$$

where, $D$ is the diameter of the soil-covering and soil-compacting wheel, cm; $f$ is the friction coefficient between soil and soil-covering and soil-compacting wheel, $f = 0.5$; $Q$ is the gravity of the soil-covering and soil-compacting wheel and its additional load, N; $W_r$ is the friction torque in the shaft sleeve, N ·m.

The friction torque in the shaft sleeve is:

$$W_r = \frac{1}{2}uPd \tag{7}$$

where, $\mu$ Is the friction coefficient of rolling bearing, $\mu$= 0.2; $P$ is the bearing load of rolling bearing, N; $d$ is the shaft diameter length of rolling bearing, cm.

According to the shaft diameter length $d$ of 4.6 cm and the bearing load force $P$ of rolling bearing is 320 N, the friction torque $W_r$ in the shaft sleeve could be obtained from Equation (7) as 147.2 N·cm. Generally, the friction torque in the shaft sleeve would be expanded by 10 times (about 1472 N·cm) to overcome the increased friction caused by the entry of dust or solid substances during operation. According to Equation (6), the diameter $D$ of the soil-covering and soil-compacting wheel was greater than or equal to 18.4 cm. Combined with practical experience, the diameter range of the soil-covering and soil-compacting wheel was generally 20-50 cm[28]. Then, according to the flatness of the soil-covering and soil-compacting soil in the field, the rolling resistance in the operation process was reduced under the condition of smooth rotation and reduced backwater, and the diameter $D$ of the designed sharp angle soil-covering and soil-compacting wheel was 20 cm.

### 2.3.2 Design of tip angle parameters and length

Through the analysis of the principle of soil-covering and soil dynamics, it could be seen that the factors affecting the suppression effect, the amount of soil-covering and the direction of soil movement were the distance from the tip of the sharp angle to the surface of the drum, that is, the sharp angle height $h$ and the sharp angle $\alpha$, as agronomy required that the soil-covering thickness should be controlled at about 1 cm, and considered that the soil-covering and soil-compacting wheel had a certain suppression effect on the soil, so that the soil and Panax notoginseng seeds sank to a certain extent, the sharp angle height $h$ was designed to be 0.8-1.6 cm; Sharp angle $\alpha$ Through the analysis of the corresponding angle of the lower limit, as shown in Figure 6, the sharp angle increased, and the final resultant force $F_T$ gradually moved downward. The sharp angle should meet the requirement that the resultant force points to the seed ditch, so the maximum angle is 105°-120°. Considering that some soil at the bottom of the ridge could slide into the seed ditch, 105° was selected as the maximum angle of the sharp angle, and the sharp angle was 45°-105°.

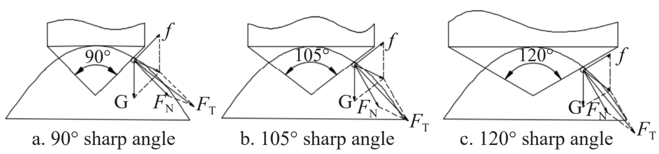


a. 90° sharp angle b. 105° sharp angle c. 120° sharp angle

Figure 6 Analysis of lower limit angle of sharp angle

The length of the soil-covering and soil-compacting wheel was related to the width of furrow, ridge width and sowing row spacing.

The row plant spacing required by Panax notoginseng agronomy was 5 cm and the soil-covering thickness was 1 cm. Because the final sowing depth was affected by the soil fall during furrow opening and the soil disturbance during soil-covering and soil-compacting, the effect was better when the furrow depth was 2 cm. If the distance between the sharp angles of the soil-covering and soil-compacting wheel was about equal to the sowing row spacing, the length of the soil-covering and soil-compacting wheel is:

$$B = nL + b \tag{8}$$

where, $L$ is the sowing row spacing, cm; $n$ is the number of rows; $b$ is the width of sharp angle, cm. The sowing row spacing of Panax notoginseng is 5 cm. According to the sharp angle height and angle range, the sharp angle width $b$ is 0.7-4.1 cm, so the length of the soil-covering and soil-compacting wheel of the two rows of planting ditch is 10.7-14.1 cm.

2.3.3 Design of pressure regulating structure

During the working process of the soil-covering and soil-compacting, it was necessary to ensure that the soil-covering and soil-compacting wheel rolls forwarded with the fluctuation of the surface soil, and met certain requirements of soil compactness. Therefore, the ballast pressure regulating part was required to control the ballast pressure to meet the agronomic requirements of the soil compactness of Panax notoginseng seedling. When the soil-covering and soil-compacting wheel covered and pressed the soil on the soft soil after humidity regulation and leveling, the ground bears the load imposed by the soil-covering and soil-compacting wheel, and the soil would sink to a certain extent, that is, the lower limit $Z_0$[29]:

$$Z_0 = \frac{6Q}{5KBD^{\frac{1}{2}}} \tag{9}$$

where, $Z_0$ is the lower limit, mm; $B$ is the length of the soil-covering and soil-compacting wheel, mm; $D$ is the diameter of the soil-covering and soil-compacting wheel, mm; $Q$ is the total load of the soil-covering and soil-compacting wheel, N; $K$ is the soil characteristic parameter; $\alpha_0$ is parameter related to soil properties; Among them $K = \alpha_0$ (1+0.27$B$); For the soft soil just after humidity regulation and leveling, take $\alpha_0$= 1.4[2]. Through the above formula, the relevant parameters of the soil-covering and soil-compacting wheel are brought into the lower limit formula, and the total load of the soil-covering and soil-compacting wheel on the soil can be calculated to be about 705.42 N.

By weighing, the gravity of the soil-covering and soil-compacting device was about 320 N, and the force provided by the compression spring of the profiling adjustment structure was about 385.42 N. according to the spring force formula:

$$\Delta F = k\Delta x \tag{10}$$

According to Equation (10), the spring stiffness value is 38.54 N/mm, query the relevant national standards (GB2089-2009 ordinary cylindrical helical compression spring dimensions and parameters), and select YA4×25×60 GB/T2089 compression spring.

## 3 Simulation analysis of soil-covering and soil-compacting wheel

From the above theoretical analysis, it could be seen that different sharp angle angles and heights had an important impact on the force of seeds and the effect of soil-covering and soil-compacting. In order to further clarify the influence law of sharp angle parameter changes on seed disturbance and soil-covering thickness, the discrete element method was used to simulate and analyze the process of soil-covering and soil-compacting, so as to determine the range of structural parameters.

### 3.1 Simulation model establishment

Use SolidWorks 2018 software to establish the model of soil-covering and soil-compacting wheel, as shown in Figure 7a. During the simulation, the value range of sharp angle and sharp angle height was 45°-105° and 0.8-1.6 cm respectively according to the previous research. The forward speed of soil-covering and soil-compacting wheel was consistent with the speed of the planter, specifically 10 m/min. The soil trough model and test process were shown in Figures 7b and 7c. The three-dimensional size of the soil trough model was 15 cm×16 cm×3.5 cm, because a single row could not represent the stress and compression between seed ditches, two rows of seed ditch models were designed, and the stress and displacement of one seed were calculated in each row. However, considering the deviation of the first seed and excluding the contingency, one seed was added before and after each row, with 3 seeds in each row, a total of 6 seeds. The soil matrix adopted 1 mm particles, and the seed adopts multi ball polymerization model, with a diameter of 5.75 mm. In reference [30,31], the surface energy of soil JKR was 4.31 J/m$^2$, the soil-soil recovery coefficient, static friction coefficient and dynamic friction factor were 0.4, 0.7 and 0.07 respectively, and the soil-covering and soil-compacting wheel recovery coefficient, static friction coefficient and dynamic friction coefficient were 0.3, 0.6 and 0.1, respectively.

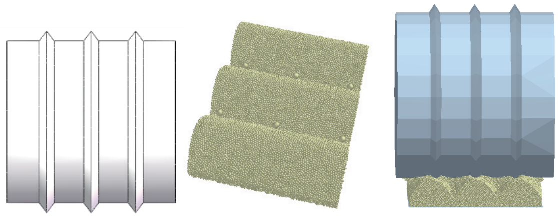

a. Model of wheel b. Model of soil trough c. Simulation test process

Figure 7 Establishment of simulation model

### 3.2 Simulation results and analysis

3.2.1 Stress analysis of seeds

In the process of soil-covering and soil-compacting, the force on the seed would affect the final soil-covering and soil-compacting effect. Therefore, when the sharp angle height and angle were 0.8-1.6 cm and 45°-105° respectively, the normal force on the seed was analyzed, and the result value was taken as the force mean value of 6 seeds. In order to observe the force uniformity, the variance of the normal force was analyzed. The test results are shown in Figures 8 and 9.

It could be seen from Figure 8 that the normal force received by the seed increases from 0 to 0.65 s, reached the peak at about 0.6 s, and decreased after 0.65 s. Comparing the peak value of normal force on Seeds under different sharp angle height, it could be seen that the change rate and peak value of normal force on seeds increase with the increase of sharp angle height; Compared different sharp angles, the change rate and peak value of normal force were the smallest at 45°, the maximum at 105°, and the change rate and peak value of normal force were similar at 60°-90°. It could be seen from Figure 9 that under different sharp angle heights, the variance value of normal force showed an upward trend, and the variance value increased gently when the sharp angle height was 0.8-1.2 cm; Under different sharp angle, the change of square difference was relatively small when the angle was 45°-90°, indicated that the

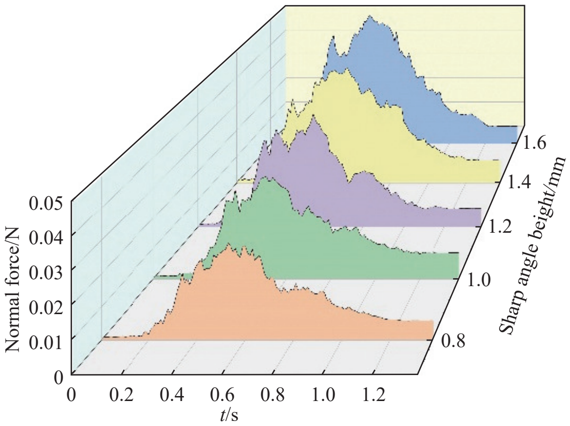


a. different sharp angle heights

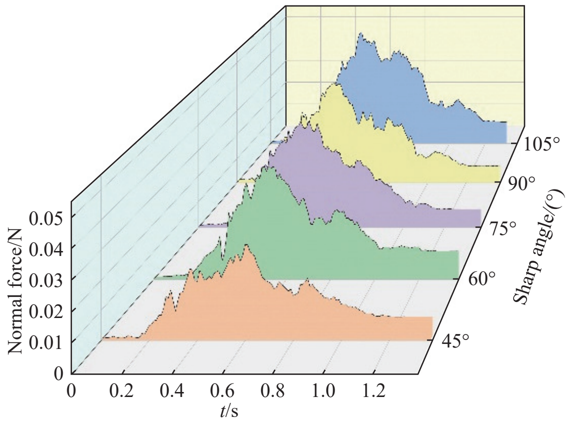


b. different sharp angle angles

Figure 8 Normal stress waterfall of seed

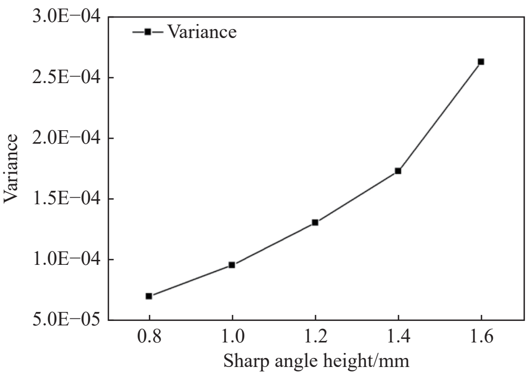


a. Different sharp angle height

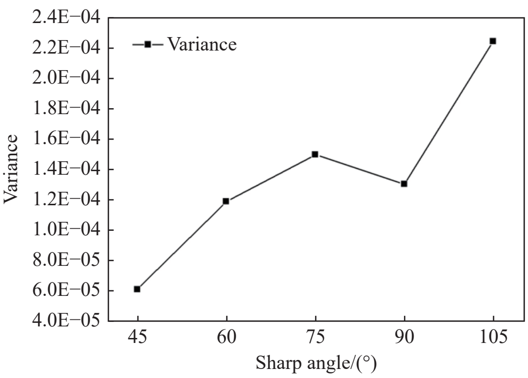


b. different sharp angle

Figure 9 Analysis of variance of normal force

normal force uniformity of seeds was relatively good.

3.2.2 Analysis of soil-covering effect

The angle and height of the sharp angle were selected as the test factors, and the soil-covering thickness and seed offset were taken as the test indexes. The single factor test was carried out to determine the best range of the height of the sharp angle, so as to provide a reference basis for the orthogonal combination test below. The simulation results are shown in Figure 10.

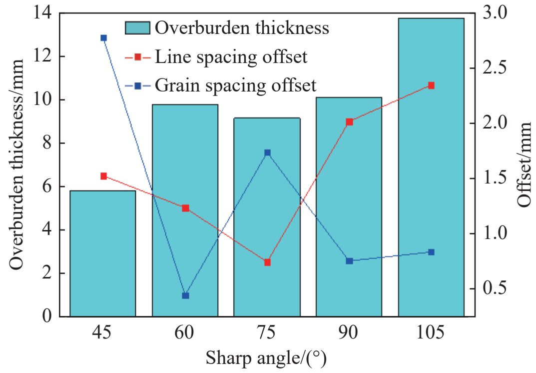


a. different sharp angle

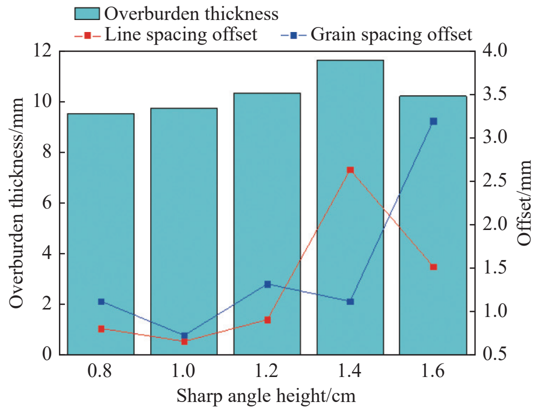


b. different sharp angle height

Figure 10 Analysis of soil-covering performance

It could be seen from Figure 10a that when the sharp angle was 60°, 75° and 90°, the change of soil-covering thickness was small and the thickness was stable at about 1 cm, which met the agronomic requirements of soil-covering thickness, and the deviation of grain spacing and row spacing was relatively small; It could be seen from Figure 10b that the soil-covering thickness under different sharp angle heights met the requirements. From the analysis of row spacing and grain spacing offset of Panax notoginseng seeds, the seed offset increased with the increase of sharp angle height. When the sharp angle height was 0.8, 1 and 1.2 cm, the seed offset was small and stable at 1 mm left and right; In conclusion, according to the analysis of the influence of different sharp angle and height on the soil-covering thickness and seed offset, when the sharp angle and height were 60°-90° and 0.8-1.2 cm respectively, the overall soil-covering and soil-compacting effect was better than other conditions, met the agronomic requirements of Panax notoginseng seedling and sowing.

## 4 Performance test of soil-covering and soil-compacting wheel

### 4.1 Test purpose

In order to explore the operation parameters with good soil-covering and soil-compacting effects, the Box-Behnken Design test with four factors and three levels was carried out with the forward speed of the planter, spring ballast, the sharp angle and height of the soil-covering and soil-compacting wheel as the test factors and the soil-covering thickness, grain spacing and soil compactness as the test indexes to optimize the structural parameters with the best operation effect.

## 4.2 Test materials and equipment

The test was carried out on the soil trough frame of the machining training center of Yunnan Agricultural University. The length, width and thickness of the soil trough are 12 000 mm, 1500 mm and 300-350 mm, respectively, and the soil moisture content was 20%. The soil trough test was shown in Figure 11. The main instruments and equipment used in the test are: Panax notoginseng seedling seeding precision planter, soil-covering and soil-compacting device (soil-covering and soil-compacting wheel was processed by 3D printing technology, 9 groups of Soil-covering and soil-compacting wheels were assembled according to the test level), soil moisture meter, soil compactness instrument, humidity spray device, shovel, steel ruler, tape measure, etc.


1. Soil-covering and soil-compacting wheel 2. Panax notoginseng seedling seeding precision planter 3. Soil trough

Figure 11 Soil trough test

## 4.3 Test plan and method

According to the principle of Box-Behnken Design combination design, the orthogonal combination test of four factors and three levels was carried out. The levels of test factors are listed in Table 1. According to the orthogonal combination test design, the test design scheme included 24 groups of factorial points and 5 groups of zero point tests. The test scheme and results are listed in Table 2. After the test, the regression processing and analysis of the test results were carried out by using Design Expert 10.0.7 software to obtain the analysis of variance and Regression equation and response surface analysis.

**Table 1 Test factors and levels**

| Level | factors | | | |
|---|---|---|---|---|
| | Forward speed/m·min$^{-1}$ | Ballast pressure/N | Sharp angle/(°) | Sharp angle height/cm |
| 1 | 6 | 280 | 60 | 0.8 |
| 0 | 8 | 415 | 75 | 1.0 |
| –1 | 10 | 550 | 90 | 1.2 |

## 4.4 Analysis of variance and response surface method

### 4.4.1 Analysis of variance of test indexes

After the test data were fitted by quadratic regression, the regression equation of test factors on test indexes after soil-covering and soil-compacting was obtained, and the corresponding analysis of variance are listed in Tables 3-5. After excluding insignificant factors, the regression equation was as follows:

$$y_1 = 3.92 - 0.34x_1 - 0.056x_3 + 0.33x_4 + 0.000\,26x_3^2 \tag{11}$$

$$y_2 = -2.43 + 3.59x_4 + 0.000\,67x_2x_3 + 0.031x_1^2 - (7.08E-6)x_2^2 - 0.001x_3^2 - 2.88x_4^2 \tag{12}$$

**Table 2 Test plan and results**

| Level | Forward speed $x_1$/ m·min$^{-1}$ | Ballast pressure $x_2$/N | Sharp angle $x_3$/(°) | Sharp angle height $x_4$/cm | Soil-covering thickness/ cm | Grain spacing/ cm | Soil compactness/ kPa |
|---|---|---|---|---|---|---|---|
| 1 | 10 | 550 | 75 | 1.0 | 0.57 | 4.88 | 272.56 |
| 2 | 6 | 550 | 75 | 1.0 | 0.56 | 4.51 | 279.24 |
| 3 | 10 | 280 | 75 | 1.0 | 0.57 | 4.61 | 298.47 |
| 4 | 6 | 280 | 75 | 1.0 | 0.58 | 4.82 | 333.60 |
| 5 | 8 | 415 | 90 | 1.2 | 0.54 | 5.08 | 244.22 |
| 6 | 8 | 415 | 60 | 1.2 | 0.62 | 4.63 | 279.33 |
| 7 | 8 | 415 | 90 | 0.8 | 0.51 | 4.91 | 204.76 |
| 8 | 8 | 415 | 60 | 0.8 | 0.61 | 4.75 | 345.73 |
| 9 | 10 | 415 | 75 | 1.2 | 0.54 | 5.03 | 267.42 |
| 10 | 6 | 415 | 75 | 1.2 | 0.71 | 4.95 | 283.02 |
| 11 | 10 | 415 | 75 | 0.8 | 0.51 | 5.10 | 305.33 |
| 12 | 6 | 415 | 75 | 0.8 | 0.62 | 4.92 | 355.38 |
| 13 | 8 | 550 | 90 | 1.0 | 0.63 | 4.92 | 252.40 |
| 14 | 8 | 280 | 90 | 1.0 | 0.51 | 4.62 | 239.82 |
| 15 | 8 | 550 | 60 | 1.0 | 0.52 | 4.63 | 373.98 |
| 16 | 8 | 280 | 60 | 1.0 | 0.47 | 5.12 | 310.07 |
| 17 | 10 | 415 | 90 | 1.0 | 0.67 | 4.80 | 244.91 |
| 18 | 6 | 415 | 90 | 1.0 | 0.71 | 4.72 | 259.00 |
| 19 | 10 | 415 | 60 | 1.0 | 0.47 | 4.92 | 317.62 |
| 20 | 6 | 415 | 60 | 1.0 | 0.83 | 4.68 | 243.39 |
| 21 | 8 | 550 | 75 | 1.2 | 0.61 | 4.77 | 274.58 |
| 22 | 8 | 280 | 75 | 1.2 | 0.49 | 4.92 | 295.51 |
| 23 | 8 | 550 | 75 | 0.8 | 0.50 | 4.59 | 304.18 |
| 24 | 8 | 280 | 75 | 0.8 | 0.61 | 4.62 | 259.87 |
| 25 | 8 | 415 | 75 | 1.0 | 0.43 | 4.45 | 253.33 |
| 26 | 8 | 415 | 75 | 1.0 | 0.62 | 4.59 | 221.28 |
| 27 | 8 | 415 | 75 | 1.0 | 0.57 | 4.65 | 245.91 |
| 28 | 8 | 415 | 75 | 1.0 | 0.64 | 4.58 | 226.06 |
| 29 | 8 | 415 | 75 | 1.0 | 0.51 | 5.00 | 333.91 |

**Table 3 Variance analysis of soil-covering thickness**

| Variance source | Sum of squares | freedom | Mean square sum | $F$ | $p$ |
|---|---|---|---|---|---|
| Model | 0.140 00 | 8 | 0.018 00 | 5.74 | 0.0007 |
| $x_1$ | 0.046 00 | 1 | 0.046 00 | 14.60 | 0.0011 |
| $x_2$ | 0.004 91 | 1 | 0.004 91 | 1.57 | 0.2246 |
| $x_3$ | 0.029 00 | 1 | 0.029 00 | 9.28 | 0.0064 |
| $x_4$ | 0.020 00 | 1 | 0.020 00 | 6.40 | 0.0199 |
| $x_1 x_3$ | 0.011 00 | 1 | 0.011 00 | 3.53 | 0.0751 |
| $x_2 x_4$ | 0.004 90 | 1 | 0.004 90 | 1.57 | 0.2250 |
| $x_1^2$ | 0.014 00 | 1 | 0.014 00 | 4.39 | 0.0492 |
| $x_3^2$ | 0.023 00 | 1 | 0.0230 | 7.51 | 0.0126 |
| Residual | 0.063 00 | 20 | 0.031 20 | | |
| Spurious term | 0.050 00 | 16 | 0.003 12 | 0.99 | 0.5683 |
| Pure error | 0.013 00 | 4 | 0.003 15 | | |
| The sum | 0.210 00 | 28 | | | |

$$y_3 = -2010.13 + 189.37x_1 + 1.7x_2 - 99.23x_1x_4 - 1.41x_2x_4 - 0.001x_2^2 - 0.12x_3^2 \tag{13}$$

According to the results of variance analysis in Table 3, the $p$-value of the soil-covering thickness model was 0.0007<0.01, indicated that the model formula was very significant. It was known from the $p$-value that the test factors $x_1$ and $x_3$ had a very significant impact on the soil-covering thickness, $x_4$, $x_1^2$ and $x_3^2$ had a significant impact on the soil-covering thickness, and other factors had no significant impact on the soil-covering thickness. The order of the

**Table 4 Analysis of variance of grain spacing**

| Variance source | Sum of squares | freedom | Mean square sum | *F* | *P* |
|---|---|---|---|---|---|
| Model | 0.700 | 10 | 0.070 | 4.10 | 0.0046 |
| $x_1$ | 0.031 | 1 | 0.031 | 1.81 | 0.1950 |
| $x_2$ | 0.057 | 1 | 0.057 | 3.37 | 0.0829 |
| $x_3$ | 8.33E-006 | 1 | 8.33E-006 | 4.893E-004 | 0.9826 |
| $x_4$ | 0.088 | 1 | 0.088 | 5.15 | 0.0358 |
| $x_1 x_4$ | 0.031 | 1 | 0.031 | 1.80 | 0.1966 |
| $x_2 x_3$ | 0.076 | 1 | 0.076 | 4.44 | 0.0494 |
| $x_1^2$ | 0.100 | 1 | 0.100 | 5.98 | 0.0250 |
| $x_2^2$ | 0.110 | 1 | 0.110 | 6.35 | 0.0214 |
| $x_3^2$ | 0.350 | 1 | 0.350 | 20.43 | 0.0003 |
| $x_4^2$ | 0.086 | 1 | 0.086 | 5.07 | 0.0371 |
| Residual | 0.310 | 18 | 0.017 | | |
| Spurious term | 0.280 | 14 | 0.020 | 3.09 | 0.1423 |
| Pure error | 0.260 | 4 | 6.480E-003 | | |
| The sum | 1 | 28 | | | |

**Table 5 Variance analysis of soil compactness**

| Variance source | Sum of squares | freedom | Mean square sum | *F* | *p* |
|---|---|---|---|---|---|
| Model | 29 581.11 | 10 | 2958.11 | 2.61 | 0.0366 |
| $x_1$ | 6379.17 | 1 | 6379.17 | 5.63 | 0.0289 |
| $x_2$ | 5754.49 | 1 | 5754.49 | 5.08 | 0.0369 |
| $x_3$ | 597.70 | 1 | 597.70 | 0.53 | 0.4768 |
| $x_4$ | 399.05 | 1 | 399.05 | 0.35 | 0.5601 |
| $x_1 x_4$ | 6301.18 | 1 | 6301.18 | 5.57 | 0.0298 |
| $x_2 x_3$ | 3317.18 | 1 | 3317.18 | 2.93 | 0.1041 |
| $x_2 x_4$ | 5803.39 | 1 | 5803.39 | 5.13 | 0.0362 |
| $x_1^2$ | 3853.38 | 1 | 3853.38 | 3.40 | 0.0816 |
| $x_2^2$ | 5530.38 | 1 | 5530.38 | 4.88 | 0.0403 |
| $x_3^2$ | 5150.41 | 1 | 5150.41 | 4.55 | 0.0470 |
| Residual | 20 378.98 | 18 | 1132.17 | | |
| Spurious term | 16 010.85 | 14 | 1143.63 | 1.05 | 0.5380 |
| Pure error | 4368.13 | 4 | 1092.03 | | |
| The sum | 49 960.08 | 28 | | | |

influence degree of the test factors on the soil-covering thickness from large to small is: forward speed $x_1$, sharp angle $x_3$, sharp angle height $x_4$ and ballast $x_2$.

According to the results of analysis of variance in Table 4, the *p*-value of grain spacing model was 0.0046<0.01, indicated that the model was very significant. According to the *p*-value, the effect of test factor $x_4^2$ on grain spacing was very significant, $x_4$, $x_2 x_3$, $x_1^2$, $x_2^2$ and $x_3^2$ were significant, and other factors had no significant effect on grain spacing. The influence degree of test factors on particle spacing from large to small was as follows: sharp angle height $x_4$, ballast pressure $x_2$, forward speed $x_1$ and sharp angle $x_3$.

According to the results of analysis of variance in Table 5, the *p*-value of soil compactness model was 0.0366<0.05, indicating that the model was significant. According to the *p*-value, the test factors $x_1$, $x_2$, $x_1 x_4$, $x_2 x_4$, $x_2^2$, $x_3^2$ had significant effects on soil compactness, and other factors had no significant effects on soil compactness. The influence degree of test factors on soil compactness from large to small is: forward speed $x_1$, ballast pressure $x_2$, sharp angle $x_3$ and sharp angle height $x_4$.

4.4.2 Response surface analysis

The response surface method was used to analyze the influence of the four test factors on the three indicators. From Tables 3-5, it could be seen that the interaction of test factors $x_2x_3$ had a significant impact on the grain spacing, and the interaction of test indicators $x_1x_4$ and $x_2x_4$ had a significant impact on the soil compactness. Therefore, the response surface method was used to analyze it, and the response surface was obtained, as shown in Figure 12.

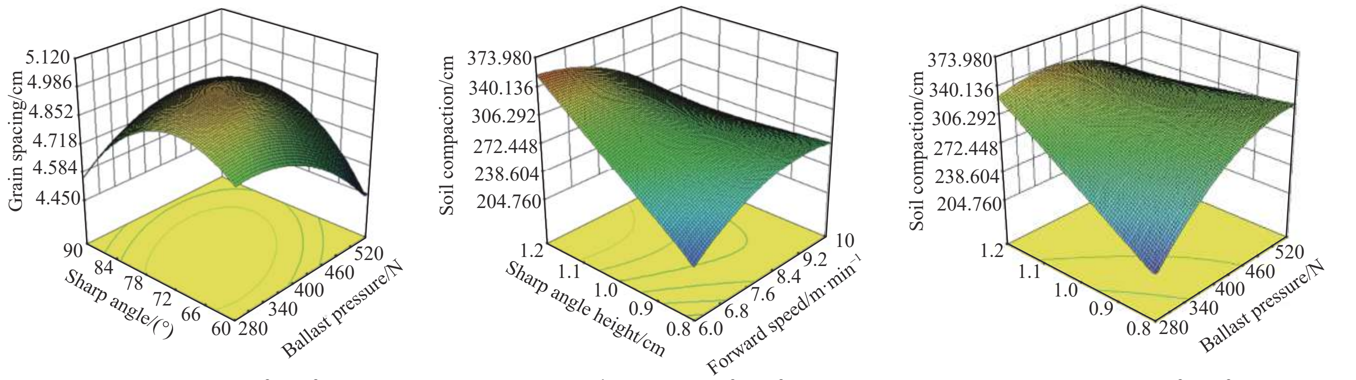


a. Response surface of $x_3 x_2$ to grain spacing

b. Response surface of $x_4 x_1$ to soil compactness

c. Response surface of $x_4 x_2$ to soil compactness

Figure 12 Response surface of test factors to indicators

It could be seen from Figure 12a that the grain spacing first increased and then decreased with the increase of ballast pressure, and also increased and then decreased with the increase of sharp angle. When the ballast pressure and sharp angle were in the middle area, the value of grain spacing was closest to 5 cm, and the effect of sowing grain spacing was better. It can be seen from Figure 12b that the soil compactness gradually increased with the decrease of forward speed and the increase of sharp angle height. With the increase of sharp angle height, the forward speed gradually increased between 6-8.4 m/min and slightly decreased between 8.4-10 m/min; It could be seen from Figure 12c that the soil compactness basically increased first and then decreased with the increase of ballast pressure, increased gradually between 280-400 N and decreases gradually between 400-550 N with the increase of sharp angle height.

4.4.3 Optimization of test parameters

In order to obtain the best working parameters of soil-covering thickness, grain spacing and soil compactness, taken the forward speed, ballast pressure, sharp angle and sharp angle height as independent variables and the optimal soil-covering thickness, grain spacing and soil compactness as the goal, the best working parameter combination of the planter was obtained by analyzing the results of the quadratic orthogonal combination test with the data analysis software Design-Expert 10: the forward speed was 6.5 m/min, ballast pressure was 360.51 N, sharp angle was 67.39° The height of the sharp angle was 1.03 cm. Under this condition, the soil-covering thickness reached 0.66 cm, the grain spacing reached 4.6 cm, and the soil compactness reached 303.05 kPa.

### 4.5 Verification test of test results

In order to further verify the soil-covering and soil-compacting performance under the best parameters, the verification test was carried out according to the best parameter combination. Considered the actual processing conditions, the best parameter values are rounded. The forward speed was 6.5 m/min, the ballast pressure was 360.5 N, the sharp angle was 67°, and the sharp angle height was 1 cm. The test site is shown in Figure 13.

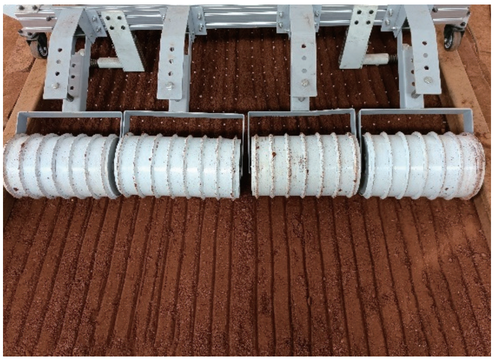

Figure 13 Soil-covering and soil-compacting process

In order to eliminate random errors, three groups of tests were carried out, and the average values of the three groups of test indexes were taken to obtain the comparison test results, as listed in Table 6.

**Table 6 Test verification results**

| Test type | Soil-covering thickness/cm | Grain spacing/cm | Soil compactness/kPa |
|---|---|---|---|
| Software analysis value | 0.66 | 4.60 | 303.05 |
| Test verification value | 0.64 | 5.03 | 321.77 |
| Error/% | 3.03 | 9.35 | 6.18 |

The experimental verification results showed that the soil-covering thickness of Panax notoginseng seedling planter was 0.64 cm, the grain spacing was 5.03 cm, the soil compactness was 321.77 kPa, and the error was within 10%, which was basically consistent with the software analysis results. The operation effect met the agronomic requirements of Panax notoginseng seedling sowing, and the best parameter combination could provide guidance for production practice.

## 5 Conclusions

1) According to the special agronomic requirements of shallow sowing depth and dense seed ditches of Panax notoginseng, a sharp angle roller soil-covering and soil-compacting device was designed. Through the rolling calculation of soil-covering and soil-compacting wheel, the movement of soil particles and the analysis of the subsidence of soil-compacting wheel, it is determined that the diameter of soil-covering and soil-compacting wheel was 20 cm, the sharp angle height range was 0.8-1.6 cm, the sharp angle range was 45°-105°, and the maximum stiffness of spring was 38.54 N/mm.

2) The simulation analysis of seed stress, soil-covering and soil-compacting effect under different sharp angle height and angle was carried out, and the sharp angle parameter range of soil-covering and soil-compacting wheel was further determined. The results showed that when the sharp angle height range was 0.8-1.2 cm and the sharp angle range was 60°-90°, the seed stress uniformity, soil-covering and soil-compacting effect were relatively good.

3) Taken the forward speed, ballast pressure, sharp angle and sharp angle height as the test factors and the soil-covering thickness, grain spacing and soil compactness as the indexes, the four factor and three-level orthogonal combination test was carried out, and the soil-covering and soil-compacting performance under the best parameters is verified through the whole machine test. The results showed that when the forward speed was 6.5 m/min, the ballast pressure was 360.5 N, the sharp angle was 67° and the sharp angle height was 1 cm, the soil-covering thickness the grain spacing and soil compactness were 0.64 cm, 5.03 cm and 321.77 kPa respectively, which met the agronomic requirements of seedling raising and sowing of Panax notoginseng. The research could provide guidance for production practice.

## Acknowledgements

The authors acknowledge that this work was financially supported by the National Natural Science Foundation of China (Grant No. 32160425), the Joint Special Key Project for Agriculture of Yunnan Science and Technology Plan (Grant No. 2018FG 001-007) and the Major Science and Technology Project of Yunnan Province (Grant No. 202102AE090042-06-04).

## [References]

[1] Intelligent research consultation. Analysis on planting area, output and main trade areas of Panax notoginseng in China in 2021.https://baijiahao.baidu.com/s?id=1706315442668453736&wfr=spider&for=pc, 2022.3.

[2] Yang W C, Pu W, Pan W J, Zhang X W, Zhang L, Zheng J X. Design and experiment of soil-covering and compacting device for Panax notoginseng seedling sowing. Journal of South China Agricultural University, 2022; 43(2): 122–132. (in Chinese)

[3] Yang W C, Zhu Y Y, Du Q, Xi Q. Engineering and technology system analysis on pseudo-ginseng industrial seedling production in Yunnan. Journal of Southern Agriculture, 2012; 43(12): 2069–2073. (in Chinese)

[4] Berti M T, Johnson B L, Henson A. Seeding depth and soil packing affect pure live seed emergence of cuphea. Industrial Crops and Products, 2008; 27(3): 272–297.

[5] Bassegio D, Santos R F, Secco D, Zanão L A, Werncke I, Sarto M V M. Short-term effects of crop rotations on soil chemical properties under no-tillage condition. Australian Journal of Crop Science, 2015; 9(1): 49–54.

[6] Haruna S I, Nkongolo N V. Influence of cover crop, tillage, and crop rotation management on soil nutrients. Agriculture. 2020; 10(6): 225.

[7] Altikat S, Celik A. The effects of tillage and intra-row compaction on seedbed properties and red lentil emergence under dry land conditions. Soil & Tillage Research, 2011; 114(1): 1–8.

[8] Cheţan F, Cheţan C, Rusu T, Şimon A. Effects of the winter wheat cultivation in tillage system without plowing on the soil properties. Ards Turda, 2015; 8(22): 119–125.

[9] Sawant C K P, Kumar A, Mani I, Singh J K, Yadav R, Sahoo R N. Performance evaluation of IARI wheat seed-cum-fertilizer plot drill for pearl millet-wheat cropping system on permanent raised bed system. Journal of Agricultural Engineering, 2019; 55(4): 1–12.

[10] Guo H, Chen Z, Jia H L, Zheng T Z, Wang G, Wang Q. Design and experiment of soil-covering and soil-compacting device with cone-shaped structure of wheel. Transactions of the CSAE, 2017; 33(12): 56–65. (in Chinese)

[11] Zhang Z J, Sun X W, Jin Z N, Bing Z, Sun Q Y, Tong J. Design and test of crushing bionic soil-covering device of soybean seeder. Transactions of the CSAM, 2018; 49(2): 34–40, 73. (in Chinese)

[12] Zheng Z Q, Fu Z L, Wang C Y, Huang Y X, He J P. Design and experimental research on soil-covering device with linkage and differential adjustment of potato planter. Agriculture, 2021; 11(7): 665–665.

[13] Li K, Li S Z, Teng X, Deng Z L, Huang W B, Gan F F, et al. Integrated design and evaluation of a soil-covering and film-mulching device for sugarcane transverse planters. Agronomy, 2021; 11(7): 1382–1382.

[14] Bi S Y, Liu W D, Guo L J. Dynamic analysis and parameter optimization of coupled bionic press roller on soybean ridge. Journal of Chinese Agricultural Mechanization, 2020; 41(9): 25–32. (in Chinese)

[15] Liu H J, Zhao S H, Tan H W, Yang Y Q, Zhang X M. Investigation on press device in reducing adhesion and resistance based on scrape and vibration principle. Transactions of the CSAM, 2018; 49(1): 86–92. (in Chinese)

[16] Tong J, Zhang Q Z, Chen D H, Chang Y, Wang H C. Effects of bionic geometric structure press rollers on reducing rolling resistance and adhesion against soil. Applied Mechanics and Materials, 2013; 461: 63–72.

[17] Jia H L, Guo H, Guo M Z, Wang L C, Zhao J L, Fan X H. Finite element analysis of performance on elastic press wheel of row sowing plow machine for covering with soil and its experiment. Transactions of the CSAE, 2015; 31(21): 9–16, 315. (in Chinese)

[18] Fukami K, Mukunoki T, Nakano K, Matsuo N, Okayasu T. Water leakage control by using vibratory roller on a dry-seeded rice field in southwestern Japan. Soil & Tillage Research, 2017; 166: 138–146.

[19] Inano I, Momono H, Suzuki T, Arita T. Study on improving the emergence of direct sowing sugar beets (Part 1): Improving emergence rate by press roller attached to seeder. Journal of the Japanese Society of Agricultural Machinery, 2006; 68(6): 75–82.

[20] Taser O F, Kara O. Silage maize (*Zea mays* L. ) seedlings emergence as influenced by soil compaction treatments and contact pressures. Plant Soil & Environment, 2006; 51(7): 289–295.

[21] Tang Q, Wu C Y, Yuan W S, Wu J, Wang S F. Structure design on compacting and covering soil device of rape shallow transplanting machine. Journal of Chinese Agricultural Mechanization, 2016; 37(3): 20–22, 33.

[22] Li M, Xu S, Yang Y W, Guo L, Tong J. A 3D simulation model of corn stubble cutting using finite element method. Soil & Tillage Research, 2017; 166: 43–51.

[23] Bentaher H, Ibrahmi A, Hamza E, Hbaie M, Kantchev G, Maalej A, et al. Finite element simulation of moldboard–soil interaction. Soil and Tillage Research, 2013; 134(8): 11–16.

[24] Ahmad F, Qiu B J, Ding Q S, Ding W M, Khan Z M, Shoaib M, et al. Discrete element method simulation of disc type furrow openers in paddy soil. Int J Agric & Biol Eng, 2020; 13(4): 103–110.

[25] Li L Y, Gong X, Xu T, Guo P. Simulation analysis of soil-covering process. Journal of Physics:Conference Series, 2020; 1578: 012099.

[26] Sun J F, Chen H M, Wang Z M, Yang Z, Liu Z, Duan J L. Study on plowing performance of EDEM low-resistance animal bionic device based on red soil. Soil & Tillage Research, 2020; 196: 104336–104336.

[27] Koolen A J, Kuipers H. Agricultural soil mechanics. Springer Science & Business Media, 2012.

[28] Agricultural Machinery Design Manual. Beijing: China Agricultural Science and Technology Press, 2007. (in Chinese)

[29] Yang W C, Xu L L, Du Y F, Lang C C, Pan W J. Design and experiment of the pressing wheel profiling ditching device for sowing panax notoginseng to grow seedlings. Transactions of the CSAE, 2020; 36(7): 53–62. (in Chinese)

[30] Xiang W, Wu M L, Lv J N, Quan W, Ma L, Liu J J. Calibration of simulation physical parameters of clay loam based on soil accumulation test. Transactions of the CSAE, 2019; 35(12): 116–123. (in Chinese)

[31] Xing J J, Zhang R, Wu P, Zhang X R, Dong X H, Chen Y, et al. Parameter calibration of discrete element simulation model for latosol particles in hot areas of Hainan Province. Transactions of the CSAE, 2020; 36(5): 158–166. (in Chinese)